Bioorganic & Medicinal Chemistry 17 (2009) 5688–5695

Contents lists available at ScienceDirect

Bioorganic & Medicinal Chemistry

journal homepage: www.elsevier.com/locate/bmc

# Antimicrobial and immunomodulatory properties of prenylated xanthones from twigs of *Garcinia staudtii*

Joseph Ngoupayo [a,*], Turibio Kuiate Tabopda [b], Muhammad Shaiq Ali [c]

[a] Département de Pharmacie et Pharmacothérapeutique Africaine, Faculté de Médecine et des Sciences Biomédicales, Université de Yaoundé 1, BP 1364 Yaoundé, Cameroun
[b] Département de Chimie Organique, Université Yaoundé I, BP 812 Yaoundé, Cameroun
[c] H.E.J. Research Institute of Chemistry, University of Karachi, Karachi-75270, Pakistan

ARTICLE INFO

*Article history:*
Received 8 March 2009
Revised 30 May 2009
Accepted 5 June 2009
Available online 13 June 2009

*Keywords:*
Clusiaceae
*Garcinia staudtii*
Xanthones
Antibacterial activity
Immunomodulatory activity

ABSTRACT

Phytochemical investigation of the methanol extract of the twigs of *Garcinia staudtii* yielded four new prenylated xanthones, staudtiixanthones A–D (**1**–**4**), along with eleven known compounds. Their structures were determined by analysis of 1D and 2D NMR spectra and by comparison of spectroscopic data with those previously reported. Some of these compounds have been evaluated for antibacterial activity against methicillin-resistant *Staphylococcus aureus* (MRSA). The new compounds were also screened for phagocyte chemiluminescence, neutrophil chemotaxis, T-cell proliferation, cytokine production from mononuclear cells and cytotoxicity. They were found to exhibit potent immunomodulatory activities.



## 1. Introduction

Immunomodulation is a very broad term which denotes any changes in the immune response and may involve induction, expression, amplification or inhibition of any part or phase of the immune response. Modulation may be very specific limited to a given antigen/agent or non-specific, with a general effect on immune response. Stimulation of the immune response is desired for certain people such as immunocompromised patient, whereas suppression of the immune response is thought for others, such as transplant recipient, allergic and inflammatory diseased patients.[1] Natural compounds with potential immunostimulating activity studied can be classified as high and low molecular weight compounds. These compounds belong to different classes of substances. Terpenoids, phenolic compounds, and alkaloids dominate among low molecular weight compounds, and polysaccharides dominate among the high molecular weight compounds.

*Garcinia staudtii* is a morphologically distinctive species of flowering plant in the Clusiaceae family. It is confined to forested areas extending from south-east Nigeria to Cameroon.[2] Medicinal plants of the genus *Garcinia* are known to be rich in prenylated xanthones.[3] Xanthone constituents have been reported to possess several biological activities, such as antibacterial, antimalarial, radical scavenging, cytotoxicity, inhibition of cyclooxygenase, and prostaglandin E2 activities.[4–8] In our continuing phytochemical investigation of *Garcinia* plants found in Cameroon, we have examined the twigs of *G. staudtii*. To our knowledge, no chemical investigation of *G. staudtii* has been reported. This investigation led to the isolation and structural elucidation of four new prenylated xanthones (**1**–**4**) and eleven known compounds; friedelin, lupeol, α- and β-amyrin, β-sitosterol, stigmasterol, α-mangostin (**5**),[9] garcinone B (**7**),[9] demethylcalabaxanthone (**6**),[10] Gartanin (**8**),[11] and xanthone $V_1$ (**9**).[12] The isolated xanthones were tested for their antimicrobial activities against methicillin-resistant *Staphylococcus aureus* (MRSA). New xanthones **1**–**4** were also evaluated for their immunomodulatory properties.

## 2. Results and discussion

### 2.1. Chemistry

The $CHCl_3$ fraction of the twigs of *G. staudtii* were subjected to repeated column chromatography to yield four new prenylated xanthones (**1**–**4**) together with friedelin, lupeol, α- and β-amyrin, β-sitosterol, stigmasterol and five known xanthones (**5**–**9**) (Fig. 1).

Staudtiixanthone A (**1**), obtained as a colorless amorphous powder, showed a $[M]^+$ peak at *m/z* 396.1563 in the HREIMS, corresponding to a molecular formula of $C_{23}H_{24}O_6$. The IR spectrum showed the presence of hydroxyl groups (3401–3448 $cm^{-1}$), a chelated carbonyl group (1647 $cm^{-1}$), and benzene rings (1587, 1558, and 1513 $cm^{-1}$). The UV (MeOH) spectrum exhibited characteristic

* Corresponding author. Tel.: +92 237 96853797; fax: +92 237 22221873.
*E-mail address:* jngoupayo@yahoo.fr (J. Ngoupayo).

0968-0896/$ - see front matter © 2009 Elsevier Ltd. All rights reserved.
doi:10.1016/j.bmc.2009.06.009

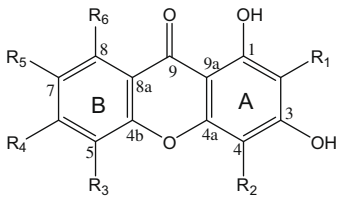

**1** $R_1 = R_2$ = prenyl; $R_3 = R_5$ = OH; $R_4 = R_6$ = H
**5** $R_1 = R_6$ = prenyl; $R_2 = R_3$ = H; $R_4$ = OH; $R_5 = OCH_3$
**8** $R_1 = R_2$ = prenyl; $R_3 = R_6$ = OH; $R_4 = R_5$ = H

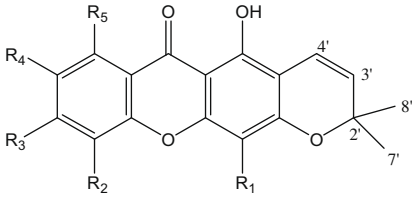

**2** $R_1$ = prenyl; $R_2 = R_4$ = OH; $R_3 = R_5$ = H
**6** $R_1 = R_2 = R_3$ = H; $R_4$ = OH; $R_5$ = prenyl
**9** $R_1 = R_4 = R_5$ = H; $R_2 = R_3$ = OH

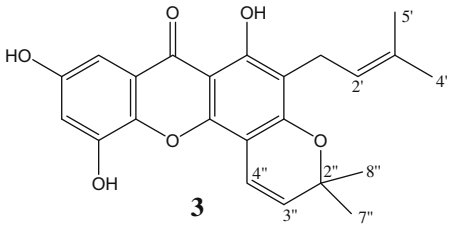

**3**

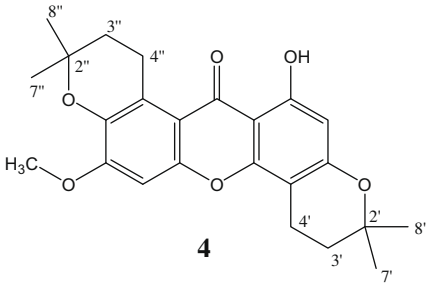

**4**

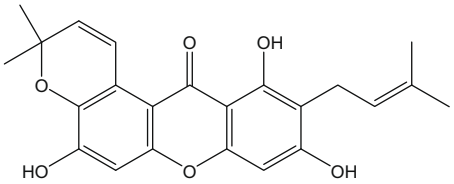

**7**

**Figure 1.** Chemical structures of isolated xanthones **1**–**9** from *Garcinia staudtii*.

absorption bands of the xanthone[13] at $\lambda_{max}$ 246, 276, 308, and 338 nm. $^1$H and $^{13}$C NMR data (Table 1), aided by DEPT and HMQC experiments, disclosed the presence of a carbonyl, twelve sp$^2$ quaternary carbons (six of which were oxygen bearing), four sp$^2$ methines, two sp$^3$ methylenes, and four methyl groups. The initial analysis of the NMR spectral data of **1** indicated the presence of a xanthone skeleton and two prenyl moieties. The $^1$H NMR spectrum (Table 1) showed a pair of two *meta*-aromatic proton signals at $\delta_H$ 6.15 (1H, d, $J$ = 1.9 Hz) and 6.47 (1H, d, $J$ = 1.9 Hz) as well as a chelated hydroxyl signal at $\delta_H$ 13.34 (1H, s). In addition, typical signals of two prenyl groups [four allylic methyl groups at $\delta_H$ 1.69 (3H, s, $H_3$-5″), 1.70 (3H, s, $H_3$-5′), 1.73 (3H, s, $H_3$-4′), and

**Table 1**
$^1$H and $^{13}$C NMR data of **1**, **2**, **3**, and **4** at 400 MHz (for $^1$H NMR) and 100 MHz (for $^{13}$C NMR) in $CDCl_3$, $\delta$ in ppm, $J$ in hertz

| Position | 1 | | 2 | | 3 | | 4 | |
|---|---|---|---|---|---|---|---|---|
| | $^{13}$C | $^1$H | $^{13}$C | $^1$H | $^{13}$C | $^1$H | $^{13}$C | $^1$H |
| **1** | 160.4 | | 156.7 | | 160.9 | | 163.9 | |
| **2** | 107.9 | | 105.5 | | 111.9 | | 100.1 | 6.24 s |
| **3** | 156.1 | | 158.1 | | 159.0 | | 161.6 | |
| **4** | 106.2 | | 109.0 | | 102.4 | | 101.0 | |
| **4a** | 162.9 | | 155.2 | | 150.9 | | 159.7 | |
| **4b** | 136.4 | | 136.4 | | 136.4 | | 139.6 | |
| **5** | 146.4 | | 146.1 | | 146.2 | | 100.3 | 6.83 s |
| **6** | 102.0 | 6.15 d (1.9) | 101.9 | 6.15 d (2.1) | 101.9 | 6.15 d (2.0) | 150.9 | |
| **7** | 156.7 | | 156.7 | | 156.7 | | 140.1 | |
| **8** | 106.3 | 6.47 d (1.9) | 106.3 | 6.51 d (2.1) | 106.3 | 6.50 d (2.0) | 120.4 | |
| **8a** | 129.1 | | 128.9 | | 128.8 | | 110.7 | |
| **9** | 179.5 | | 179.9 | | 179.8 | | 187.9 | |
| **9a** | 104.6 | | 104.3 | | 104.3 | | 100.9 | |
| **1′** | 21.3 | 3.32 br d (7.1) | | | 21.5 | 3.32 br d (7.8) | | |
| **2′** | 121.7 | 5.09 t (7.1) | 78.8 | | 122.9 | 5.25 t (7.8) | 75.1 | |
| **3′** | 134.4 | | 127.6 | 5.78 d (10.2) | 131.5 | | 32.9 | 1.73 t (6.8) |
| **4′** | 18.1 | 1.73 s | 116.6 | 7.03 d (10.2) | 18.1 | 1.79 s | 23.2 | 2.79 t (6.8) |
| **5′** | 25.5 | 1.70 s | | | 25.8 | 1.65 s | | |
| **7′, 8′** | | | 28.0 | 1.47 s | | | 26.4 | 1.39 s |
| **1″** | 22.1 | 3.25 br d (6.8) | 21.7 | 3.34 br d (7.4) | | | | |
| **2″** | 121.5 | 5.13 t (6.8) | 122.9 | 5.19 t (7.4) | 78.6 | | 75.9 | |
| **3″** | 134.9 | | 131.4 | | 127.5 | 5.81 d (10.3) | 31.7 | 1.88 t (6.8) |
| **4″** | 18.0 | 1.75 s | 18.0 | 1.80 s | 116.5 | 7.11 d (10.3) | 16.9 | 3.47 t (6.8) |
| **5″** | 25.7 | 1.69 s | 25.9 | 1.65 s | | | | |
| **7″, 8″** | | | | | 28.3 | 1.49 s | 26.7 | 1.31 s |
| OH | | 13.34 s | | 13.47 s | | 13.47 s | | 12.78 s |
| $OCH_3$ | | | | | | | 55.8 | 3.61 s |

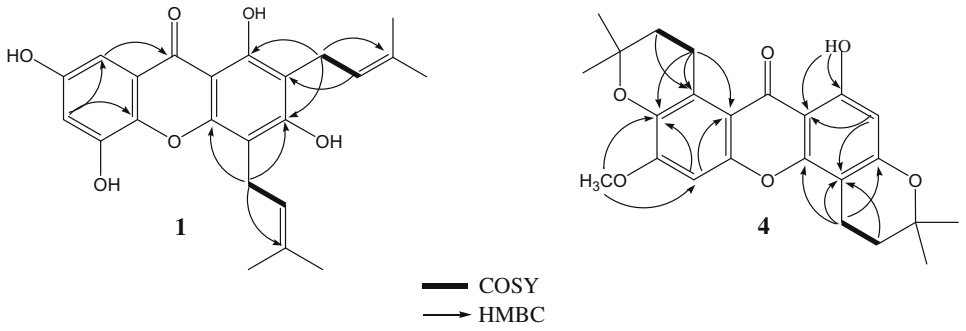


**Figure 2.** Selected COSY and HMBC correlations for compounds **1** and **4**.

1.75 (3H, s, $H_3$-4″); two pairs of methylene protons at $\delta_H$ 3.25 (2H, br d, $J$ = 6.8 Hz, $H_2$-1″) and 3.32 (2H, br d, $J$ = 7.1 Hz, $H_2$-1′); and two olefinic protons at $\delta_H$ 5.09 (1H, t, $J$ = 7.1 Hz, H-2′) and 5.13 (1H, t, $J$ = 6.8 Hz, H-2″)] were observed in the $^1$H NMR spectrum of **1**. The six substituents on the xanthone skeleton were determined on the basis of the HMBC spectral analysis (Fig. 2). The locations of the two prenyl moieties were placed at the C-2 ($\delta_C$ 107.9) and C-4 ($\delta_C$ 106.2) positions by the HMBC correlations of $H_2$-1′/C-1 ($\delta_C$ 160.4), $H_2$-1′/C-2, and $H_2$-1′/C-3 ($\delta_C$ 156.1), and $H_2$-1″/C-3, $H_2$-1″/C-4 and $H_2$-1″/C-4a ($\delta_C$ 162.9) in the HMBC spectrum of **1** (Fig. 2), respectively. The substitution pattern of ring B was elucidated by the interrelated peaks of H-6/C-4b ($\delta_C$ 136.4), H-6/C-5 ($\delta_C$ 146.4), H-6/C-8 ($\delta_C$ 106.3), H-8/C-6 ($\delta_C$ 102.0), H-8/C-4b, and H-6/C-9 ($\delta_C$ 179.5) in the HMBC spectrum. Therefore, three hydroxyl groups were positioned to the C-5, C-7 ($\delta_C$ 156.7), and C-1 positions, and the remaining two oxygen-bearing quaternary carbons were assigned to the C-4a and C-4b positions, respectively. These results established the structure of staudtiixanthone A (**1**) as 1,3,5,7-tetrahydroxy-2,4-diprenylxanthone.

Staudtiixanthone B (**2**), which is obtained as a colorless amorphous powder, has a molecular formula $C_{23}H_{22}O_6$ based on the results of HREIMS ($m/z$ 394.1411). The IR spectrum showed absorption bands for hydroxyl and conjugated ketone functional groups. The UV spectrum of **2** exhibited bands very similar to those of **1**. The $^1$H and $^{13}$C NMR spectra (Table 1) aided by DEPT and HMQC experiments disclosed the presence of 23 carbons that were arranged similarly to those of **1**, except for the replacement of one prenyl group with a 2,2-dimethylpyran ring [$\delta_H$ 1.47 (6H, s), 5.78 and 7.03 (1H, each, d, $J$ = 10.2 Hz)]. The presence of the 2,2-dimethylpyran moiety was further confirmed both by the $^{13}$C NMR spectrum which showed characteristic signals at $\delta_C$ 28.0 (C-5′, C-6′), 78.8 (C-2′), 116.6 (C-4′), and 127.6 (C-3′)[14] and by the EIMS on which the base peak at $m/z$ 379 $[M-15]^+$ was observed. As in (**1**), the $^1$H NMR spectrum of (**2**) (Table 1) showed the characteristic signals of two *meta*-aromatic protons [$\delta H$ 6.15 (1H, d, $J$ = 2.1 Hz) and $\delta_H$ 6.51 (1H, d, $J$ = 2.1 Hz)] located on the ring B. There remained the placement of the dimethylpyran ring and the prenyl group. In the HMBC spectrum, the proton resonating at $\delta_H$ 7.03 (H-4′) was correlated with oxygenated aromatic carbons at $\delta_C$ 156.7 (C-1) and 158.1 (C-3) through $^3J$, which implied that the dimethylpyran ring oxygen belongs to the hydroxyl group at C-3. Hence, from the above analysis, the 2,2-dimethylpyran and prenyl groups were concluded to be located at C-2/C-3 and C-4, respectively. The chemical shifts of C-1 to C-4a were in agreement with those reported for inoxanthone.[15] The structure of staudtiixanthone B (**2**) was, therefore, concluded to be 1,5,7-trihydroxy-4-prenyl-2′,2′-dimethylpyrano[5′,6′:2,3]xanthone.

Staudtiixanthone C (**3**) was isolated as a colorless amorphous powders and gave the same molecular formula $C_{23}H_{22}O_6$ as (**2**) by HREIMS ($[M]^+$ at $m/z$ 394.1409). Both compounds displayed similar NMR features (Table 1), UV absorption bands, and the same fragmentation patterns in the EIMS, suggesting that **2** and **3** were isomers. The $^1$H NMR, $^{13}$C NMR, HSQC, HMBC, and $^1$H–$^1$H COSY spectra revealed the presence of one dimethylpyran ring, one prenyl group, and one hydrogen-bonded hydroxy group. Comparison of the $^{13}$C NMR spectral data with those of **2** revealed a significative difference mainly for the carbon shifts at ring A. The HMBC correlations observed for **3** were in perfect agreement with an angular arrangement of the pyrano unit. In this respect, the HMBC spectrum showed correlations between the proton resonating at $\delta_H$ 3.32 (2H, br d, $J$ = 7.8 Hz, H-1′) and aromatic carbons at $\delta_C$ 160.9 (C-1) through $^3J$, which suggested the placement of the prenyl group at C-2. Strong NOE interaction observed between the prenyl protons at $\delta_H$ 3.32 ($H_2$-1′) and chelated proton at $\delta_H$ 13.47 (1-OH) in the NOESY spectrum further supported the placement of the prenyl group at C-2 and the 2,2-dimethylpyran ring at C-3/C-4, with the furan ring oxygen at C-3. On the basis of the above data, the structure of staudtiixanthone C (**3**) was assigned as 1,5,7-trihydroxy-2-prenyl-2′,2′-dimethylpyrano[5′,6′:3,4]xanthone.

Staudtiixanthone D (**4**) was obtained as yellow amorphous powder. It was formulated as $C_{24}H_{26}O_6$ on the basis of its HREIMS ($[M]^+$ ($m/z$ 410.1727). Its IR spectrum exhibited vibration bands due to hydroxyl (3454 $cm^{-1}$) and conjugated carbonyl (1647 $cm^{-1}$) groups. The UV absorptions (237, 260, 321, and 360 nm) indicated (**4**) to be a xanthone derivative. The $^1$H NMR of (**4**) revealed the presence of one chelated hydroxyl group at $\delta_H$ 12.78 (1H, s, 1-OH), one methoxyl group at $\delta_H$ 3.61 (3H, s), two isolated aromatic protons at $\delta_H$ 6.24 (1H, s) and 6.83 (1H, s), and two 2,2-dimethylchroman rings [$\delta_H$ 3.47, 2.79 (2H each, t, $J$ = 6.8 Hz), 1.88, 1.73 (2H each, t, $J$ = 6.8 Hz), 1.39, 1.31 (6H each, s)]. The chelated hydroxyl proton (1-OH) gave a $^3J$ peak with a methine aromatic carbon at $\delta_C$ 100.1 (C-2) which was correlated to the aromatic proton ($\delta_H$ 6.24, H-2) in the HMQC spectrum. A dimethylchroman ring was then located at C-3/C-4. This was confirmed by HMBC correlations of H-2 ($\delta_H$ 6.24)/C-9a, H-2/C-4 ($\delta_C$ 101.0), H-4′ ($\delta_H$ 2.79)/C-3 ($\delta_C$ 161.6), and H-4′/C-4a ($\delta_C$ 159.7). The location of the singlet aromatic proton ($\delta_H$ 6.83), the methoxyl group ($\delta_H$ 3.61), and the dimethylchroman unit in the B ring was established by HMBC correlations. Particularly noticeable feature was the highly deshielded position of the methylene protons of a 2,2-dimethylpyran unit [$\delta_H$ 1.88(H-3″) and 3.47 (H-4″)]. Such structural feature suggests this functionality to be *peri* to the carbonyl group. The methoxyl group was assigned to C-6 based on the HMBC correlations of H-5/C-4b ($\delta_C$ 139.6), H-5/C-8a ($\delta_C$ 110.7), H-5/C-7 ($\delta_C$ 140.1), and $CH_3O$/C-6 ($\delta_C$ 150.9). All assignments were compatible with the location of the 2,2-dimethylchroman units in **4**. On the basis of the above evidences, the structure of staudtiixanthone D (**4**) was elucidated as 1-hydroxy-6-methoxy-2′,2′-dimethyldihydropyrano[5′,6′:3,4]-2″,2″-dimethyldihydropyrano [5″,6″:7,8]xanthone.

**Table 2**

| Compound | 1 | 2 | 3 | 4 | 5 | 6 | 7 | 8 | 9 |
|---|---|---|---|---|---|---|---|---|---|
| MIC (μg/mL) | 16 | 32 | 128 | 64 | 32 | 128 | 128 | 32 | – |

## 2.2. Biological activity

### 2.2.1. Antibacterial activity of isolated compounds

All xanthones were tested for their antibacterial activities against MRSA. Staudtiixanthone A (**1**), B (**2**), α-mangostin (**5**), and Gartanin (**8**) exhibited a moderate activity with a MIC of 16 and 32 μg/mL while staudtiixanthones C (**3**), D (**4**), demethylcalabaxanthone (**6**), and garcinone B (**7**) showed less activity with an equal MIC value of ⩾64 μg/mL. From these results, xanthones such as **1**, **2**, **5**, and **8** with the C-4 free prenyl group had better activity than **3** and **4** with modified prenyl group at C-4. In addition, compounds **1**–**3** with the 5,7-dihydroxy groups showed a better activity than the others (Table 2).

### 2.2.2. Effect on phagocytes oxidative burst

Phagocytic cells on activation induce the release of reactive oxygen free radicals (oxidative burst), which are then quantified by a luminol-enhanced chemiluminescence assay. We investigated the inhibitory/stimulatory effects of compounds **1**–**4** on the immune system in the elimination of foreign materials. Only compound **4** showed stimulatory activity with mononuclear cells (24%), at the lower concentration (3.1 μg/mL) tested (Fig. 3a). Meanwhile at the higher concentrations of 25 and 50 μg/mL, compound **4** inhibited mononuclear cells ROS activity (59% and 70%, respectively). All tested compounds were found to have potential in suppressing phagocytosis activity of neutrophils and mononuclear cells in a dose-dependent manner (Fig. 3). However, they were less active in suppressing the activity of the monocytes compared to that of neutrophils. Compound **1**, the most active, strongly suppressed the neutrophils and mononuclear cells with activities up to 73% at 3.1 μg/mL (Fig. 3). The inhibition of the oxidative burst was not due to cytotoxic effects as none of these compounds were found to exhibit cytotoxicity.

### 2.2.3. Effect on T-cell proliferation

The anti-proliferation effect of compounds **1**–**4** was determined by measuring the inhibition of phytohemagglutinin (PHA)-induced T-cell proliferation by determining radioactive thymidine incorporation. All test compounds exhibited a strong suppressive effect on the PHA-stimulated T-cell proliferation in dose-dependent manner with $IC_{50}$ of 6.2, 6.4, 12.7, and 3.7 μg/mL, respectively (Fig. 4). A very potent and dose-dependant activity was observed with compounds **1, 2,** and **3**. Both compounds had significantly suppressed PHA T-cell proliferation activity of PBMN cells. The earlier compounds had the most potent (94.3% and 97.1%, respectively) suppressive action at 12.5 μg/mL. Compound **4** had the most potent suppressive effect on T-cell response at lower concentrations. It was found significantly active in suppressing the stimulatory action of the PHA at 3.1 μg/mL (44.9%) and 6.125 μg/mL (70.4%).

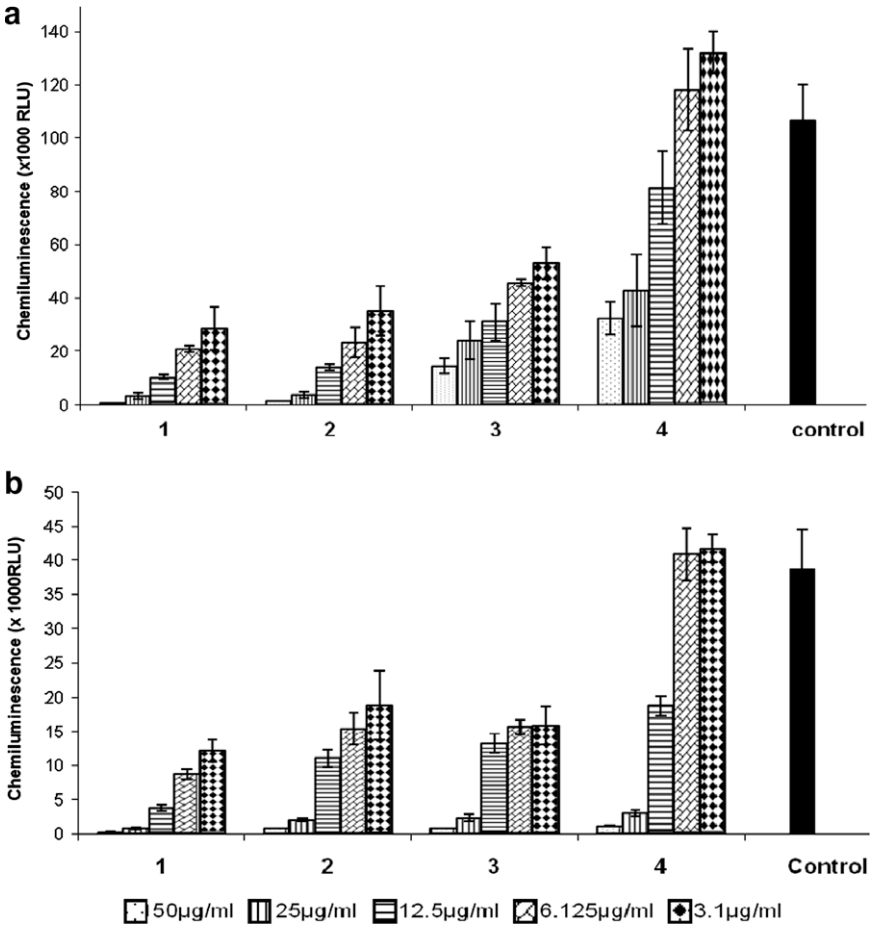


**Figure 3.** Chemiluminescence effect of compounds **1**–**4** on oxidative burst using mononuclear cells (a) and neutrophils (b). Each plot and error bar represent readings ± SD of three repeats.

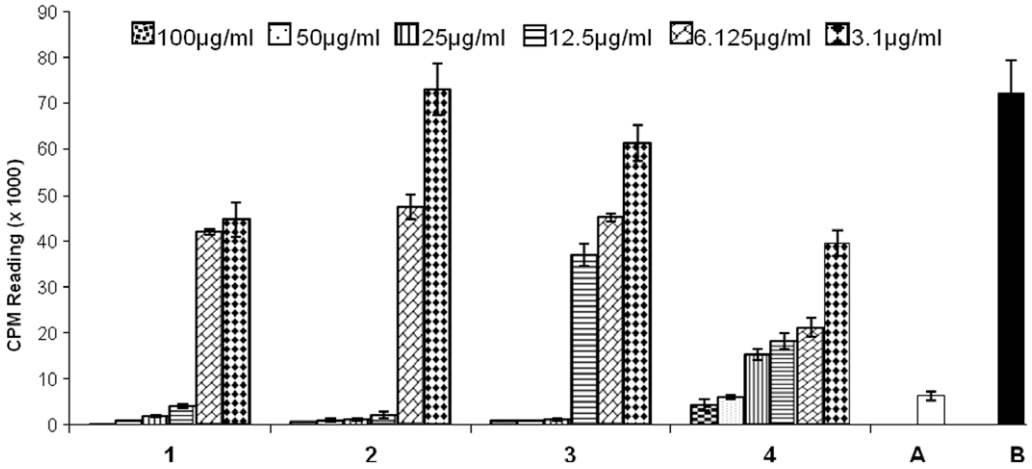


**Figure 4.** Effect of compounds on phytohemagglutinin (PHA) T-cell proliferation. The bar graph represents effect of various concentrations of the test compounds **1**–**4** after 72 h incubation with peripheral blood mononuclear cells at 37 °C. Effect of compounds on T-cell proliferation response is compared with non-proliferated (A) and proliferated (B) cells. Each bar represents the mean value of triplicate reading ± SD.

### 2.2.4. Effect on MDBK cell proliferation

When compounds **1**–**4** were evaluated for their cytotoxicity on Mavin Darby Bovine Kidney (MDBK) cells, no toxic effect was observed after 72 h of incubation (Fig. 5) at concentrations as high as 50 µg/mL. Therefore, various doses up to 50 µg/mL were used during present investigation.

### 2.2.5. Effect on cytokine release by peripheral blood mononuclear cells (PBMCs)

The suppressive effect of the compounds **1**–**4** was tested on the release of selected cytokine including IL-2, IFN-γ, and IL-4 by PHA-induced lymphocytes. Results shown in Figure 6 indicate that compounds **1**–**3** strongly inhibited IL-2, IL-4, and INF-γ release in a dose-dependent manner from PHA-activated lymphocytes. Compound **4** inhibited IL-2 and IL-4, but have less effect on the inhibition of INF-γ. Compound **1** with two unmodified prenyl groups was found to exert a very potent suppressive effect on IL-2, IFN-γ, and IL-4 production. The lowest concentration (0.5 µg) was found to be very potent in inhibiting IL-2 (68.2%) and IFN-γ (62.5%). IL-4 production was suppressed in the presence of compound **1** up to 1 µg/mL (88.1%). However, the most potent IL-4 (40.6%) suppression at low concentration (0.5 µg) was noted with compound **4**.

### 2.2.6. Effect on polymorphoneutrophil cells chemotaxis

Effect of the test compounds on PMN chemotaxis in response to a chemotactic peptide formyl-methionylleucyl-phenylalanine (fMLP $10^{-8}$) was assayed using the Boyden chambers. PMNs were incubated with three different concentrations (2.5, 5, and 25 µg/mL) of each compound for 1 h and the difference in the cell movement was studied. Prednisolone was run as a positive control. The data presented in Figure 7 show that all tested compounds exhibited potent suppressive activity on fMLP-induced PMNs movement and caused about 27–46% inhibition of chemotaxis at test concentrations, which did not change significantly with concentrations. Compound **3** had the most potent suppressive activity on chemotaxis. It exerted a very potent suppressive effect (46%) at 25 µg/mL. However with 1 h pre-incubation, potent suppression was observed at lower concentrations too (42.2% at 5 µg/mL and 36.4 at 2.5 µg/mL). A similar effect was observed with the other compounds.

## 3. Conclusions

A number of assays, which include phagocyte chemiluminescence, neutrophils chemotaxis, T-cell proliferation assay, cytokine production from mononuclear cells, and cytotoxicity evaluation were used to investigate the immunomodulating effect of new prenylated xanthones on different immune cells. The results obtained show that compounds exert inhibitory effect on phagocytic activity of PMNs and PBMCs. It was also found to interfere with the phytohemagglutinin (PHA) T-cell activation in a dose-dependant manner. The impaired incorporation of tritiated thymi-

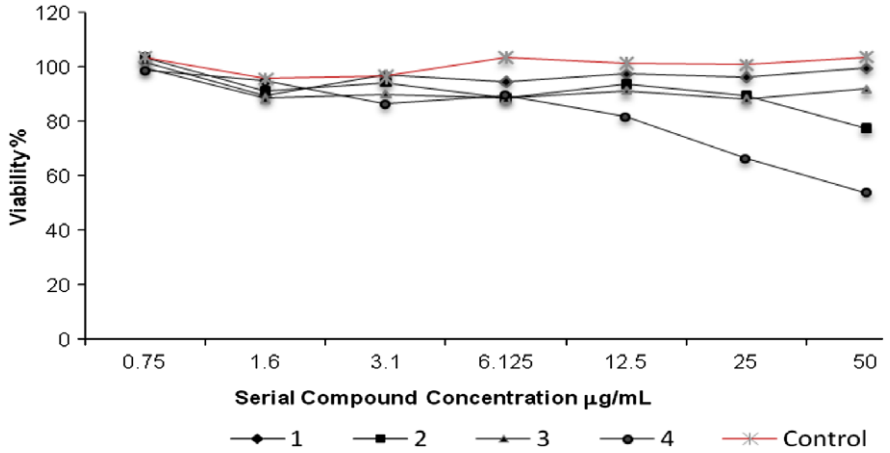


**Figure 5.** Effect of various concentrations of compounds **1**–**4** on the viability of MDBK cells after 72 h incubation. All values are the mean of three replicated.

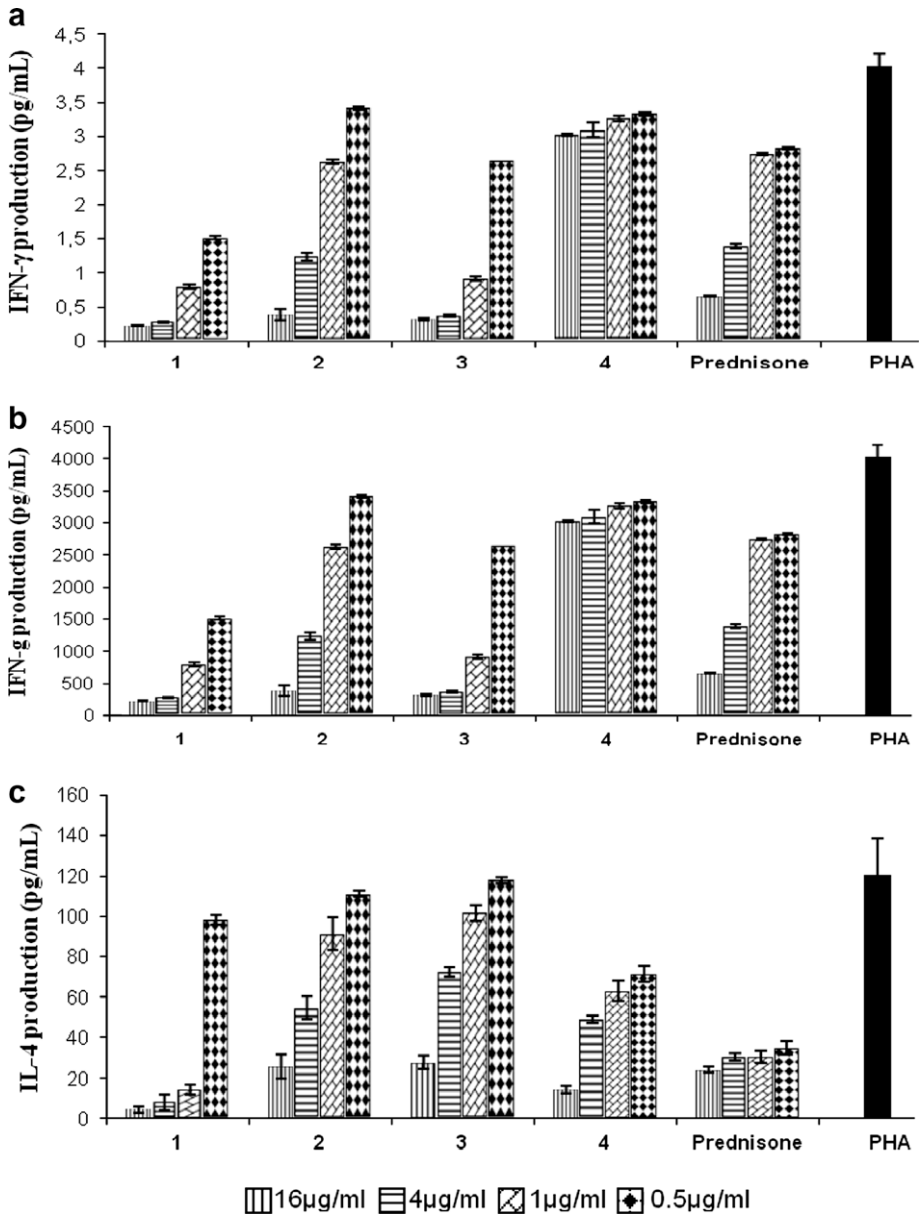


**Figure 6.** Effect of compounds **1–4** on cytokine production. Each bar represents the mean value of reading ± SD. (a) IL-2 level = 528.5 ± 34.52, (b) INF-γ level = 4033.7 ± 180, and (c) IL-4 level = 120.5 ± 18.1.

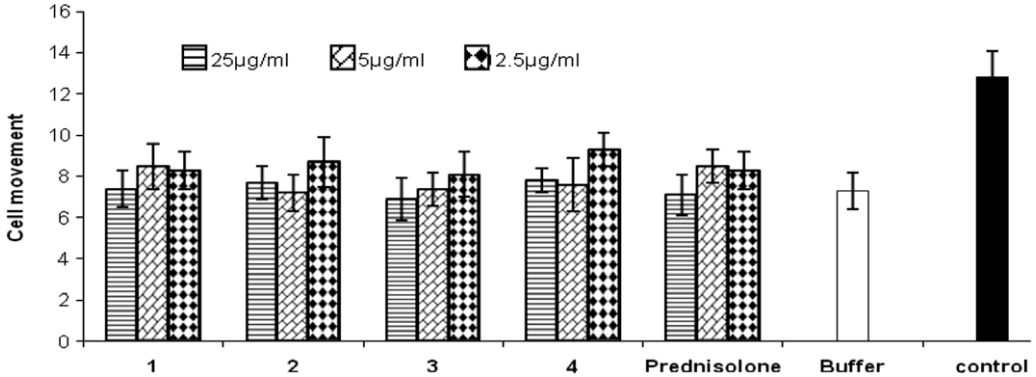


**Figure 7.** Activity comparison of compounds **1–4** with Prednisolone on Cell Movement. Buffer = no fMLP, Control = fMLP + DMSO fMLP (Formyl-Leucyl-Phenylalanine).

dine into cellular DNA may not be due to toxic effect since compounds were found to be nontoxic against MDBK cell line with a similar incubation time. The effect of compounds on T-cell proliferation was further confirmed by suppression of IL-2, IL-4, and IFN-γ production. The data presented above indicated that C-5 substitution on xanthones nucleus influences the immunosuppressive activity. The 5-OH substitution contributes in activity, while unsubstitution at this position decreases the activity. Although **1** is the most active compound of the series, the only difference between compounds is the dose concentration. A possible structural feature, which influences the activity, is the substitution pattern. Compound **1** with two free prenyl groups has better activity. The activity differences between **2** and **3** are clearly due to the presence or absence of functional groups (prenyl or dimethylpyran ring) at positions 1, 2, and 3. Compound **4** with two modified prenyl groups is the less active compound in the series in most assays. However, further mechanism-based studies are required for a better understanding of the mechanism of action of xanthones on immune response. From the results obtained, we can conclude that the testing compounds are clearly exerting immunomodulatory activity on the system used and could be suitable immunomodulatory lead compounds for future research.

## 4. Experimental

### 4.1. General

IR spectra were recorded on a JASCO 302-A spectrophotometer in $CHCl_3$. The EI-MS (ionization voltage 70 eV) was measured on a Varian AAT 311A mass spectrometer, and HR-EI-MS was taken on a JEOL HX110 mass spectrometer. 1D and 2D NMR spectra were run on Bruker AMX 400 MHz NMR spectrometer. Proton-detected heteronuclear correlations were measured using HSQC (optimized for $^1J_{CH}$ = 145 Hz) and HMBC (optimized for $J_{CH}$ = 8 Hz). The chemical shifts are given in ppm ($\delta$), relative to TMS as an internal standard, and coupling constants are expressed in hertz. Column chromatography was carried out on silica gel (70–230 mesh, Merck) and flash chromatography was carried out on silica gel (230–400 mesh, Merck). TLC was performed on Merck precoated aluminum Silica Gel 60 $F_{254}$ sheets, and compounds were detected using ceric sulfate spray reagent. A molecular device spectrophotometer was used for measurement of enzyme inhibition.

### 4.2. Plant material

The twigs of *G. staudtii* were collected in Yaounde (Mount Elunden), Center Province of Cameroon by Mr. Nana Victor (National Herbarium of Yaounde, Cameroon) in June 2008 and a voucher specimen No. HNC-167341 was deposited.

### 4.3. Extraction and isolation

The air-dried and ground twigs (1270 g) of *G. staudtii* were extracted successively with *n*-$C_6H_{14}$, $CHCl_3$, and MeOH, respectively, using a Soxhlet apparatus. After solvent removal in vacuo, the $CHCl_3$ extracts (12 g) were subjected to silica gel column, chromatography with a gradient of *n*-$C_6H_{14}$–EtOAc (5% increment of polar solvent for 500 mL of each proportion) to afford six fractions from TLC profile. Fraction 2 (3015 mg) was subjected to a silica gel column eluting with *n*-$C_6H_{14}$–EtOAc (19:1–4:1) to afford friedelin (480 mg), β-sitosterol (920 mg), stigmasterol (186 mg), lupeol (31 mg), and mixtures of α- and β-amyrin (215 mg). Fraction 3 (918 mg) was subjected to a silica gel column eluting with *n*-$C_6H_{14}$–EtOAc (3:2) to afford six major fractions, F3a–F3f. Fractions 3a (48 mg), 3b (54 mg), 3c (193 mg), and 3d (109 mg) were individually recrystallized with hexane to produce garcinone B (**7**) (7 mg), xanthone $V_1$ (**9**) (13 mg), staudtiixanthone C (**3**) (75 mg), and staudtiixanthone D (**4**) (58 mg), respectively. Fractions F3e and F3f (285 mg) were further fractionated on a silica gel column (*n*-$C_6H_{14}$–EtOAc, 1:1) and then on a Sephadex LH-20 column (in MeOH) to afford demethylcalabaxanthone (**6**) (18 mg) and α-mangostin (**5**) (13 mg). Similarly, purification of fraction 4 (1150 g) using column chromatography (silica gel, *n*-$C_6H_{14}$–EtOAc 2:3 to 3:7 in 5% increments of the EtOAc) gave staudtiixanthone A (**1**) (81 mg), staudtiixanthone B (**2**) (41 mg), and Gartanin (**8**) (9 mg) from two successive column chromatographies.

#### 4.3.1. Staudtiixanthone A (1)

Colorless amorphous powder, mp. 201 °C. UV (MeOH) $\lambda_{max}$ nm (log $\varepsilon$): 246 (4.57), 276 (3.93), 308 (3.69), 338 (3.81). IR $\nu_{max}$ (KBr) $cm^{-1}$: 3401, 3418, 3448, 1647, 1587, 1558, 1513, 1107. EIMS (probe) 70 eV, *m/z* (rel. int.): 396 $[M]^+$ (18), 381 (17), 353 (91), 341 (29), 325 (31), 327 $[M-C_5H_9]^+$ (71), 299 (100), 258 $[M-2C_5H_9]^+$ (7), 230 (21), 69 (45). HREIMS *m/z* 396.1563 (calcd for $C_{23}H_{24}O_6$: 396.1573). $^1H$ and $^{13}C$ NMR data: see Table 1.

#### 4.3.2. Staudtiixanthone B (2)

Colorless amorphous powder, mp. 214 °C. UV (MeOH) $\lambda_{max}$ nm (log $\varepsilon$): 277 (3.95), 290 (3.94), 308 (3.70), 341 (3.81). IR $\nu_{max}$ (KBr) $cm^{-1}$: 3451, 2928, 1621, 1562, 1503, 1126, 761. EIMS (probe) 70 eV, *m/z* (rel. int.): 394 $[M]^+$ (38), 379 $[M-CH_3]^+$ (61), 310 $[M-CH_3-C_5H_9]^+$ (63), 297 (100), 281 (93), (69 (43). HREIMS *m/z* 394.1411 (calcd for $C_{23}H_{22}O_6$: 394.1416). $^1H$- and $^{13}C$ NMR data: see Table 1.

#### 4.3.3. Staudtiixanthone C (3)

Colorless amorphous powder, mp. 223 °C. UV (MeOH) $\lambda_{max}$ nm (log $\varepsilon$): 289 (4.01), 307 (3.78), 341 (3.80). IR $\nu_{max}$ (KBr) $cm^{-1}$: 3440, 1621, 1560, 1499. EIMS (probe) 70 eV, *m/z* (rel. int.): 394 $[M]^+$ (38), 379 $[M-CH_3]^+$ (61), 310 $[M-CH_3-C_5H_9]^+$ (63), 297 (100), 281 (93), (69 (43). HREIMS *m/z* 394.1409 (calcd for $C_{23}H_{22}O_6$: 394.1416). $^1H$ and $^{13}C$ NMR data: see Table 1.

#### 4.3.4. Staudtiixanthone D (4)

Yellow amorphous powder. mp 208–209 °C. UV $\lambda_{max}$ (MeOH) nm (log $\varepsilon$): 237 (4.31), 260 (4.45), 321 (4.23), 360 (3.87). IR $\nu_{max}$ (KBr) $cm^{-1}$: 3454, 2943, 1647, 1608, 1511, 1149. EIMS (probe) 70 eV, *m/z* (rel. int.): 410 $[M]^+$ (26), 395 (12), 379 (63), 351 (81), 367 (100), 351 (11), 333 (21). HREIMS *m/z* 410.1727 (calcd for $C_{24}H_{26}O_6$: 410.1729). $^1H$ and $^{13}C$ NMR data: see Table 1.

### 4.4. Biological assays

#### 4.4.1. Antibacterial activity

In vitro antibacterial activity was screened against methicillin-resistant *S. aureus* (MRSA) using agar-well diffusion method.[16] 2–8 h old bacterial inoculums containing approximately $10^4$–$10^6$ colony forming units (CFU)/mL were used in these assays. The wells were dug in the media with the help of a sterile metallic borer with centers at least 24 mm. Recommended concentration (100 μL) of the test sample (1 mg/mL in DMSO) was introduced in the respective wells. The plates were incubated immediately at 37 °C for 24 h. Activity was determined by measuring the diameter of zones showing complete inhibition (mm). In order to clarify any participating role of DMSO in the biological screening, separate studies were carried out with the solutions alone of DMSO and they showed no activity against the bacterial strain.

#### 4.4.2. Chemiluminescence assay

Luminol-enhanced chemiluminescence assay was performed, as described by Helfand et al.[17] Briefly, neutrophils ($1 \times 10^7$) or

monocyte ($1 \times 10^6$), suspended in Hank's balance salt solution with calcium and magnesium ($HBSS^{++}$), were incubated with 50 μL of compounds concentrations 3.1–50 μg/mL for 30 min. To each well, 50 μl (20 mg/mL) zymosan (Sigma Chemical Co., USA), followed by 50 μl ($7 \times 10^{-5}$ M) luminol (G-9382 Sigma Chemical Co.) and then $HBSS^{++}$ was added to adjust the final volume to 0.2 mL. $HBSS^{++}$ alone was used as a control. Chemiluminescence peaks were recorded with the Luminometer (Luminoskan RS Labsystem, Finland). The luminometer was set with repeated scan mode, 50 scans with 30 s intervals and one second point measuring time. Various concentrations of compounds **1–4** were incubated with isolated polymorphoneutrophils (PMNs) and mononuclear cells (MNCs) for 30 min. The compounds activity was compared with that of the untreated samples (control) in the chemiluminescence assay.

#### 4.4.3. T-Cell proliferation assay

Peripheral blood mononuclear cells (PBMCs) were isolated from heparinized venous blood of healthy adult donor by Ficoll–Hypaque gradient centrifugation.[18] Cell proliferation was evaluated by a standard thymidine incorporation assay following a method reported by Nielsen et al.[19] Briefly, cells were cultured at a concentration of $5 \times 10^5$ cells/mL in a 96-well round-bottomed tissue culture plate (Nalge Nunc. Inter.). Cells were stimulated with 5 μg/mL of PHA (Sigma Chemical Co., USA). Various concentrations of compounds were added to obtain final concentrations of 3.1–100 μg/mL, each in triplicate. Plates were incubated for 72 h at 37 °C in 5% $CO_2$ incubator. Cultures were pulsed later with 0.5 μCi/well tritiated thymidine (Amersham Pharmacia Biotech, Sweden), and further incubated for 18 h. Cells were harvested and the tritiated thymidine incorporation was measured by a liquid scintillation counter (LS 6500, Beckman Coulter, USA). Results were expressed as mean count per minute (CPM).

#### 4.4.4. Cytotoxicity evaluation

The experiment was performed according to the method reported earlier[20] with some modification. Briefly MDBK adherent cells ($2 \times 10^5$ cells/mL) were incubated with serial concentrations of compounds (0.195–50 μg/mL) for three/five days. The supernatant was removed and 50 μl of MTT solution was then added. After 2–3 h of incubation at 37 °C, the culture medium was carefully removed, and 50 μl of 3-[4,5-dimethylthiazol-2-yl]-2,5-diphenyltetrazolium bromide (MTT) solution (2 mg/mL) was added to each well. Plates were incubated for an additional 2–3 h at 37 °C in a tissue culture incubator. After the MTT solution was aspirated off and cells were washed with phosphate buffer saline (PBS), 200 μl of DMSO was added to dissolve the blue insoluble MTT formazan produced by mitochondrial dehydrogenase. The plate was agitated at 37 °C for 15 min and then read at 540 nm using microplate readers (SpectraMax PLUS384, Molecular Devices, USA). The percentage of viable cells was calculated as the relative ratio of optical densities (ODs).

#### 4.4.5. Neutrophil chemotaxis

Chemotaxis was measured using a modified Boyden chamber (Neuro Probe, Cabin John, MD, USA), as previously described.[21] Briefly to the lower compartment 25 μL of the formyl-methionyl-leucyl-phenylalanine (fMLP) ($10^{-8}$ M) chemoattractant (Sigma Chemical Co., USA) was added. The upper compartment was separated from the lower compartment by a cellulose filter (2 μm pore size; Poretics Co., USA). To the upper compartment $5 \times 10^4$ cells in a 50 μL HBSS (with calcium and magnesium) were added. Compounds (2.5, 5, and 25 μg/mL) and control were added each in duplicate following the addition of cells. The chemoattractant buffer (DMSO and $HBSS^{++}$ without calcium and magnesium, 1:1 ratio) was added as a control. The chamber was incubated at 37 °C in $CO_2$ environment for 60 min. Cells within the filter were stained with hematoxylin and their travelling distance was measured with the help of light microscope in five randomly chosen fields per filter.

#### 4.4.6. Cytokine production from mononuclear cells

Cytokine production level was determined by ELISA Kit (Diaclone, Besancon Cedex France) and the results were recorded by ELISA reader. PBMCs were isolated from heparinized venous blood of a healthy adult donor by Ficoll gradient centrifugation. Briefly, the PBMCs were washed and suspended in RPMI-1640 supplemented with 10% AB human serum (Complete culture medium). Lymphocytes were cultured $10^5$/well in 96-well microtiter plate in the presence or absence of 1.25 μg/mL PHA. Four different concentrations (16 μg, 4 μg, 1 μg, and 0.5 μg/mL) of each compound were used in this assay. The plate was incubated for 18 h at 37 °C in a humidified atmosphere of 5% $CO_2$. After 18 h incubation, the culture plate was kept on ice and the supernatant from each well was collected carefully into small sterile Eppendorf tube that was placed on ice. The supernatant was centrifuged for 10 min at 1000*g* at 4 °C to remove particulate and aggregates. The clear supernatant from each Eppendorf tube was collected and aliquot into small volumes and kept at −20 °C till use. The supernatant was analyzed for IL-2, IL-4, and IFN-γ cytokine production.

#### 4.4.7. Statistical analysis

All data are reported as mean ± SD of the mean and the student *t*-test was used to determine the difference between test- and control preparations significance was attributed to probability values $p \leqslant 0.05$ ($p \leqslant 0.005$ in some case). The $IC_{50}$ values were calculated using Excel-based program.

## References and notes


1. Sell, S. In *Immunology, Immunopathology and Immunity*; Elsevier Science Publishing Company, Inc.: New York, 1987; pp 655–683.
2. Keay, R. W. J. In *The Trees of Nigeria*; Oxford University Press: Oxford, 1989; pp 396–397.
3. Bennett, G. J.; Lee, H. H. *Phytochemistry* **1989**, *28*, 967.
4. Rukachaisirikul, V.; Kaewno, W.; Koysomboon, S.; Phongpaichit, S.; Taylor, W. C. *Tetrahedron* **2000**, *56*, 8539.
5. Likhitwitayawuid, K.; Chanmahasathien, W.; Ruangrungsi, N.; Krungkrai, J. *Planta Med.* **1998**, *64*, 281.
6. Mahabusarakam, W.; Chairerk, P.; Taylor, W. C. *Phytochemistry* **2005**, *66*, 1148.
7. Asano, J.; Chiba, K.; Tada, M.; Yoshii, T. *Phytochemistry* **1996**, *41*, 815.
8. Nakatani, K.; Nakahata, N.; Arakawa, T.; Yasuda, H.; Ohizumi, Y. *Biochem. Pharmacol.* **2002**, *63*, 73.
9. Suksamrarn, S.; Suwannapoch, N.; Ratananukul, P.; Aroonrerk, N.; Suksamrarn, A. *J. Nat. Prod.* **2002**, *65*, 761.
10. Suksamrarn, S.; Suwannapoch, N.; Phakhodee, W.; Thanuhiranlert, J.; Ratananukul, P.; Chimnoi, N.; Suksamrarn, A. *Chem. Pharm. Bull.* **2003**, *51*, 857.
11. Parveen, M.; Khan, N. U. *Phytochemistry* **1998**, *27*, 3694.
12. Botta, B.; Monache, G. D.; Monache, F. D.; Bettolo, G. B. M.; Menichini, F. *Phytochemistry* **1986**, *25*, 1217.
13. Chaudhuri, R. K.; Ghosal, S. *Phytochemistry* **1971**, *10*, 2425.
14. Agrawal, P. K.; Bansal, M. C. In *Carbon-13 NMR of Flavonoids*; Agrawal, P. K., Ed.; Elsevier: Amsterdam, 1989; pp 83–235.
15. Yimdjo, M. C.; Azebaze, A. G.; Nkengfack, A. E.; Meyer, A. M.; Bodo, B.; Fomum, Z. T. *Phytochemistry* **2004**, *65*, 2789.
16. Carron, R.; Moran, A.; Montero, J. M.; Fernandez-Lago, L.; Dominguez, A. *Plantes Méd. Phytothér.* **1987**, *XXI*, 195.
17. Helfand, S. L.; Werkmeister, J.; Roder, J. C. *J. Exp. Med.* **1982**, *156*, 492.
18. Böyum, A. *Scand. J. Lab. Invest.* **1968**, *21*, 77.
19. Nielsen, M.; Gerwien, J.; Geisler, C.; Ropke, C.; Svejgaard, A.; Odum, N. *Exp. Clin. Immunogenet.* **1998**, *15*, 61.
20. Dimas, K.; Demetzos, C.; Marsellos, M.; Sotiriadou, R.; Malamas, M.; Kokkinopoulos, D. *Planta Med.* **1998**, *64*, 208.
21. Boyden, S. *J. Exp. Med.* **1962**, *115*, 453.